Cell Host & Microbe
Article

The Gut Commensal *Bacteroides thetaiotaomicron* Exacerbates Enteric Infection through Modification of the Metabolic Landscape

Meredith M. Curtis,[1] Zeping Hu,[2] Claire Klimko,[2] Sanjeev Narayanan,[3] Ralph Deberardinis,[2] and Vanessa Sperandio[1,4,*]
[1]Department of Microbiology
[2]Children's Medical Center Research Institute
UT Southwestern Medical Center, Dallas, TX 75390, USA
[3]Department of Diagnostic Medicine/Pathobiology, Kansas State University, Manhattan, KS 66506, USA
[4]Department of Biochemistry, University of Texas Southwestern Medical Center, Dallas, TX 75390, USA
*Correspondence: vanessa.sperandio@utsouthwestern.edu
http://dx.doi.org/10.1016/j.chom.2014.11.005

SUMMARY

The enteric pathogen enterohemorrhagic *Escherichia coli* (EHEC) causes severe diarrhea, but the influence of the gut microbiota on EHEC infection is largely unknown. A predominant member of the microbiota, *Bacteroides thetaiotaomicron* (*Bt*), is resident at EHEC attachment sites. We show that *Bt* enhances EHEC virulence gene expression through the transcription factor Cra, which is functionally sensitive to sugar concentrations. This enhanced virulence accompanies increased formation of attaching and effacing (AE) lesions requisite for EHEC colonization. Infection with *Citrobacter rodentium*, a natural mouse pathogen homologous to EHEC, in *Bt*-reconstituted mice results in increased gut permeability along with exacerbated host pathology and mortality compared to mice deplete of microflora. *Bt* modifies the metabolite environment at infection sites, increasing metabolites involved in gluconeogenesis, with stark increases in succinate, which can be sensed by Cra. Our findings suggest that microbiota composition affects disease outcome and may explain links between microbiota composition and disease susceptibility.

INTRODUCTION

Trillions of commensal bacteria inhabit the gastrointestinal tract, with the highest diversity and abundance of microbial species residing within the colon (Walter and Ley, 2011). The gut microbiota contribute to gut maturation, host nutrition, and pathogen resistance (Hooper et al., 2002; Sommer and Bäckhed, 2013), but recent findings also implicate a role for the microbiota in inflammatory bowel disease (IBD), cancer, obesity, diabetes, and heart disease (Honda and Littman, 2012; Spor et al., 2011). Multiple studies indicate that differences in microbial composition exist between healthy and diseased patients; however, it is not well understood if these shifts occur prior to disease or are a product of the disease (Gevers et al., 2014; Larsen et al., 2010; Peterson et al., 2008; Turnbaugh et al., 2009a; Turnbaugh et al., 2009b; Wang et al., 2009).

Transplantation of the microbiota from mouse strains resistant to *Citrobacter rodentium* infection rescued susceptible mice from a lethal challenge with *C. rodentium*, demonstrating that resistance could be transferred and that microbial compositions affect disease susceptibility (Willing et al., 2011). Additionally, successful treatment of recurrent *Clostridium difficile* infection through fecal transplantation further demonstrates that a balanced microbiota play an important role in preventing dysbiosis (Borody and Khoruts, 2012; Kelly et al., 2014). Specific taxa have been associated with increased disease susceptibility. A prospective study of the gut microbiota compositions in poultry workers before, during, and after exposure to *Campylobacter* found that those infected had elevated proportions of *Bacteroides* and *Escherichia* compared to those that remained uninfected despite repeated exposure (Dicksved et al., 2014).

A member of the *Bacteroidetes* phylum and major constituent of the microbiota, *Bacteroides thetaiotaomicron* encodes a number of glycoside hydrolases and polysaccharide lyases that enrich the availability of nutrients within the intestine (Sonnenburg et al., 2005). Within the intestine, *Bt* degrades complex polysaccharides into monosaccharides that can readily be used by nonglycophagic bacterial species such as *E. coli* and *C. rodentium* (Sonnenburg et al., 2005; Xu et al., 2003). Fluctuations in sugar concentrations modulate virulence gene expression and colonization of the human pathogen Enterohemorrhagic *E. coli* (EHEC) (Njoroge and Sperandio, 2012; Njoroge et al., 2012; Pacheco et al., 2012). EHEC colonizes the human colon, forming attaching and effacing (AE) lesions, invoking bloody diarrhea, hemorrhagic colitis, and hemolytic uremic syndrome (HUS). AE lesions result from extensive remodeling of the host cellular cytoskeleton that create a pedestal, or cup-like structure, beneath the bacteria (Kaper et al., 2004). EHEC also encodes a potent Shiga toxin (Stx) that is responsible for HUS (Kaper et al., 2004). EHEC intestinal colonization is dependent on the locus of enterocyte effacement (LEE) pathogenicity island (PAI) (Kaper et al., 2004). The LEE region contains five major operons (*LEE1–5*) that encode a type III secretion system (T3SS), an adhesin (intimin) and its receptor (Tir), and effector proteins (Kaper et al., 2004; Knutton et al., 1989). The *ler* gene encoded

within *LEE1* acts as the master regulator of the LEE genes (Kaper et al., 2004). Glycolytic conditions, such as those found in the gut lumen, inhibit *LEE1* expression while gluconeogenic conditions, akin to those found near the epithelial surface, activate *LEE1* expression (Njoroge and Sperandio, 2012; Njoroge et al., 2012; Pacheco et al., 2012). We sought to understand if the metabolic changes induced by *Bt* affect susceptibility to infection and disease progression of EHEC.

Our results demonstrate that *Bt* increases virulence gene expression of EHEC and *C. rodentium in vitro* and during murine infection, respectively, and that *Bt* regulation of EHEC virulence occurs through the transcription factor Cra by sensing fluctuations in sugar concentrations. Mice reconstituted with *Bt* following antibiotics treatment lost weight and succumbed to infection more rapidly than mice deplete of microflora. Perturbations to a functional T3SS or to the presence of Shiga toxin attenuated disease progression, indicating that both a functional T3SS and Shiga toxin contribute to disease. *Bt* reconstitution augments the pathophysiology associated with *C. rodentium* infection, enhancing edema of the colonic epithelium, exacerbating crypt destruction, increasing immune infiltration, and impairing intestinal epithelial repair. Additionally, we identified metabolites at sites of infection specific to *Bt* colonization, *C. rodentium* infection, or a combination of *Bt* colonization and *C. rodentium* infection. The metabolites are primarily involved in oxidative stress, nucleotide synthesis, and gluconeogenesis. Furthermore, we linked succinate, a metabolite increased at the site of infection when *Bt* is present and that has previously been shown to act as a virulence factor (Rotstein et al., 1985; Rotstein et al., 1989), with augmented secretion of the EHEC T3SS translocon. Together, our findings indicate that a prominent member of the microbiota enhances virulence gene expression of an enteric pathogen and worsens the prognosis of an enteric infection.

RESULTS

Bt Increases Expression of One-Fifth of the *E. coli* Array Probe Sets

To determine the global impact of *Bt* on EHEC gene expression, we performed a microarray from EHEC cultures grown in the presence or absence of *Bt* using the GeneChip *E. coli* Genome 2.0 array. The GeneChip *E. coli* Genome 2.0 array includes approximately 10,000 probe sets for all genes present in the following four strains of *E. coli*: K-12 lab strain MG1655, uropathogenic strain CFT073, O157:H7 enterohemorrhagic strain EDL933, and O157:H7 enterohemorrhagic strain Sakai. The microarray data represent a single replicate from each condition; therefore, no statistical analysis or multiple hypotheses testing correction was performed. Expression of one-fifth of the array probe sets increased when EHEC was cultured with *Bt* (Figure 1A). The affected genes reflect an increase in competition for nutrients, with 47% of the increased genes participating in metabolism, 8% in amino acid regulation, and 9% in cellular transport (Figure 1B). Expression of less than 1% of the EHEC genome decreased, with the most affected genes playing a role in purine and pyrimidine metabolism (Figure 1C). Despite the increase in metabolic genes, EHEC displayed no growth advantage when cultured with *Bt* (Figure 1D). However, EHEC provided a distinct growth advantage to *Bt*, increasing *Bt* generation time from 282 min/gen when grown alone to 97 min/gen when grown with EHEC (Figure 1E).

Bt Augments EHEC Virulence via the Catabolite Repressor/Activator Protein

Expression of a myriad of EHEC virulence genes is increased in the presence of *Bt*, including the LEE, *stx2a* (encoding Stx), and *stcE* (encoding a mucinase) genes (Figure 2A). The LEE PAI consists of 41 genes organized into five major operons (Kaper et al., 2004). Transcription of all LEE operons is increased when EHEC is cultured in the presence of *Bt.* In the presence of *Bt*, the master regulator of the LEE, *ler*, increased more than 3-fold ($p < 0.001$). Transcription of the T3SS structural components *escC* and *escV* increased approximately 4-fold and 3-fold, respectively (*escC:* $p < 0.0003$; *escV*: $p = 0.0319$) in the presence of *Bt* while the translocated intimin receptor *tir* increased 3-fold ($p = 0.0021$) and the T3SS filament *espA* increased 2-fold ($p = 0.05$) (Figure 2A). In accordance, AE lesion formation in EHEC significantly increased in the presence of *Bt.* In the presence of *Bt*, AE lesion formation on HeLa cells increased from 23% to 54% ($p < 0.0001$), with an increase of 8.5 pedestals per infected cell in the presence of *Bt* compared to 4.6 pedestals per cell in the absence of *Bt* (Figures 2B–2D).

To determine the pathway through which *Bt* regulates EHEC, we analyzed virulence gene expression in a panel of EHEC mutants grown in the presence or absence of *Bt.* In the presence of *Bt*, *ler* expression increased more than 3-fold in wild-type (WT) EHEC. Similarly, in the *qseC*, *qseE*, and *kdpE* EHEC mutants, *ler* expression increased approximately 3- to 4-fold when the mutants were cultured in the presence of *Bt*. In contrast, no enhancement of *ler* expression occurred in the *cra* EHEC mutant, demonstrating that *Bt* regulation of the LEE occurs through Cra, a transcription factor that positively regulates EHEC virulence by sensing fluctuations in sugar concentrations indicative of a gluconeogenic environment (Njoroge et al., 2013). *Bt* regulation does not occur through the histidine sensor kinases QseC, QseE, or FusK or through the response regulator KdpE that play other important signaling roles in EHEC virulence gene expression (Njoroge et al., 2013; Pacheco et al., 2012; Reading et al., 2007; Sperandio et al., 2002) (Figures 2E and 2F). Fluctuations in the concentrations of carbon metabolites are a major mechanism to modulate virulence gene expression and colonization of EHEC (Njoroge et al., 2013; Pacheco et al., 2012). Analysis of our microarray data corresponds with *Bt* regulation of EHEC gene expression through Cra (Figure S1 available online) (Chin et al., 1989; Feldheim et al., 1990; Saier and Ramseier, 1996).

To determine if augmentation of the LEE extends beyond *Bt* to other members of the intestinal microflora, we cultured EHEC in the presence of *Enterococcus faecalis*, a prominent member of the *Firmicutes* phyla. In the presence of *E. faecalis*, an opportunistic *Firmicutes*, transcription of all LEE operons was significantly increased (Figure 3). Transcription of *ler* increased 19-fold ($p < 0.0001$), and *escC*, *escV*, and *tir* increased 7- to 10-fold in the presence of *Bt* (*escC:* $p < 0.0001$, *escV:* $p < 0.0001$, *tir:* $p < 0.0001$), indicating that members of the two major intestinal microbiota phyla, *Bacteroidetes* and *Firmicutes*, induce the LEE in EHEC.

A

	MG1655	EDL933	Sakai	CFT073	IG	Control	Total
Increase	886	579	107	326	424	32	2354
Marginal increase	27	25	10	30	26	0	118
No change	2113	948	229	2054	797	149	6290
Marginal decrease	990	225	27	67	46	13	1368
Decrease	54	10	0	9	4	1	78
Total	4070	1787	373	2486	1297	195	10208

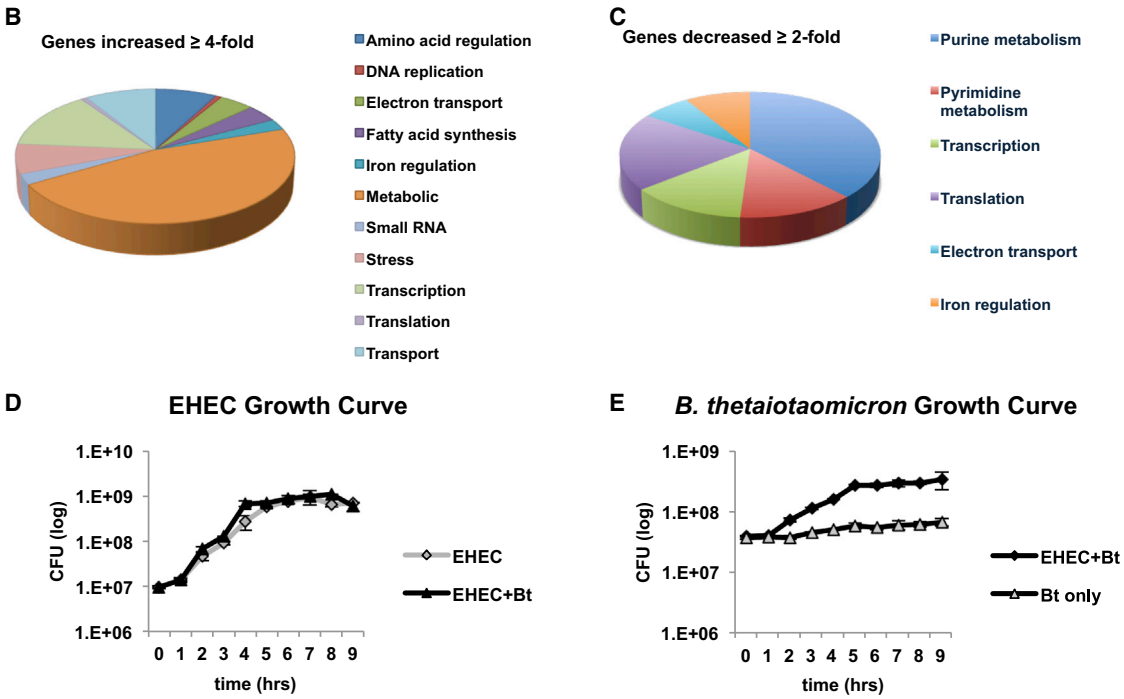

Figure 1. *B. thetaiotaomicron* (*Bt*) Increases Expression of One-Fifth of the *E. coli* Array Probe Sets

(A) Summary of microarray results comparing EHEC grown with *Bt* to EHEC grown alone (EHEC+*Bt*/EHEC only).

(B and C) Pie graph categorizing the *E. coli* genes by function (B), that increased ≥ 4-fold or (C), that decreased ≥ 2-fold in the presence of *Bt*.

(D and E) Growth curves (of six biological samples, experiments were repeated two times, each with three independent biological samples) of in vitro growth of (D) EHEC or (E) *Bt*. The error bars indicate the SD of the mean. Doubling time for EHEC grown alone and in the presence of *Bt* is 50 min/gen and 53 min/gen, respectively. Doubling time for *Bt* grown alone and in the presence of EHEC is 282 min/gen and 97 min/gen, respectively.

C. rodentium as an Infection Model

EHEC is a natural human pathogen; however, EHEC poorly infects mice, and mice do not develop key features of the disease such as AE lesions, intestinal damage, and systemic illness (Mallick et al., 2012; Mundy et al., 2005). To study the characteristics of EHEC infection, we employed an infection model using a Stx-producing *C. rodentium* strain (DBS770) constructed by Schauer and colleagues (Mallick et al., 2012). Mice infected with this strain develop AE lesions on the intestinal epithelium and Stx-dependent damage to the intestinal epithelium and kidneys (Mallick et al., 2012). In vitro analysis confirmed that *Bt* affects *C. rodentium* in a similar manner to EHEC. Similarly to EHEC, *C. rodentium* growth was unaffected by the presence of *Bt*; however, *Bt* generation time increased from 282 min/gen when grown alone to 91 min/gen when grown with *C. rodentium* (Figures 4A and 4B).

Transcription of key LEE (*ler*, *espA*, *eae*) and non-LEE encoded (*nleA* and *stx2d*) virulence genes was also increased when *C. rodentium* was grown in the presence of *Bt* (Figure 4C). Expression of *ler* increased 6-fold in the presence of *Bt* ($p = 0.0012$). Expression of *eae*, the gene that encodes the adhesin intimin essential for AE lesion formation, increased 5-fold ($p = 0.0303$), and the gene encoding the T3SS filament *espA* increased by 7.5-fold ($p = 0.0054$). *Bt* impacted *C. rodentium* growth and virulence in a similar manner to EHEC, augmenting the virulence of these AE lesion pathogens in vitro. We reasoned that *C. rodentium* would be a suitable model to study EHEC infection in the context of an altered microflora.

Bt Mediates Its Provirulence Effect on *C. rodentium* by Enhancing Expression of the T3SS, Not by a Bloom in the *C. rodentium* Population

To determine the role of *Bt* during *C. rodentium* infection in mice, mice were depleted of their microflora (Kuss et al., 2011) and then either left deplete of gut microflora or reconstituted with *Bt* (Figure S2). The mice were then challenged with a WT *C. rodentium* DBS100 strain, *C. rodentium* strain DBS770 that is Shiga toxin (Stx)+, a DBS770 Stx− (Δ*stx*), a T3SS-deficient

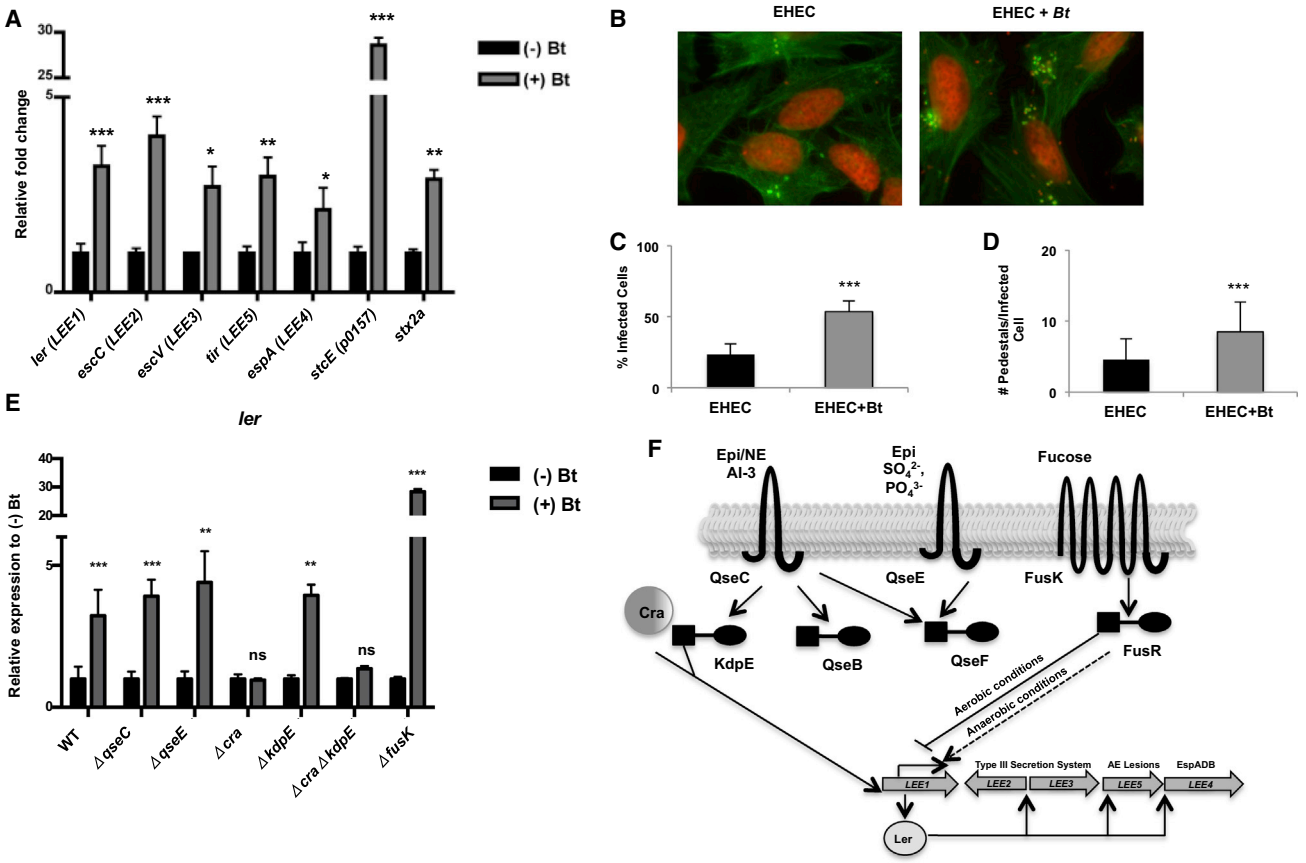

Figure 2. *Bt* Augments EHEC Virulence via the Catabolite Repressor/Activator Protein

(A) qRT-PCR of LEE, *stcE*, and *stx2A* genes in EHEC grown alone (–) *Bt* or in the presence of *Bt* (+) *Bt* (n = 9; error bars, SD; ***p < 0.001, **p < 0.01, and *p < 0.05).

(B) Fluorescent actin staining assay of HeLa cells infected with EHEC alone or in the presence of *Bt*, stained with FITC-phalloidin (actin, green) and propidium iodide (bacterial and HeLa DNA, red). Original magnification, 63×.

(C) Quantification of fluorescent actin staining assay of the percentage of HeLa cells infected, as defined by pedestal formation by EHEC.

(D) Number of pedestals/infected cell. (n = 350 cells; error bars, SD; ***p < 0.001.)

(E) qRT-PCR of *ler* in WT, *ΔqseC*, *ΔqseE*, *Δcra*, *ΔkdpE*, *ΔΔcrakdpE*, and *ΔfusK* grown alone or in the presence of *Bt* (n = 9–15; error bars, SD; ***p < 0.001, **p < 0.01, and p > 0.05 equal not significant). Each mutant has been normalized to 1 to show the fold-increase of the mutant when grown in the presence of *Bt* (+) *Bt*.

(F) Representation of LEE PAI regulation.

(Δ*escN*), or a Cra-deficient (Δ*cra*) *C. rodentium* (Figures S3 and 4). *Bt*-reconstituted mice lost weight and succumbed to *C. rodentium* infection more rapidly than microflora-deplete groups. *C. rodentium*-infected mice reconstituted with *Bt* began to lose weight on day 4 postinfection. In contrast, *C. rodentium*-infected mice deplete of microflora did not begin to lose weight until day 6 postinfection (Figure 5A). By day 6 postinfection, 50% of the *C. rodentium*-infected mice reconstituted with *Bt* had succumbed to infection, whereas only 14% of the *C. rodentium*-infected mice deplete of microflora had died by day 6 postinfection. Similarly, mice infected with *C. rodentium*Δ*stx* and reconstituted with *Bt* had 100% mortality by day 11 postinfection, while mice infected with *C. rodentium*Δ*stx* but deplete of microflora had 43% mortality on day 11 postinfection (Figure 5B). The presence of Stx compounded these effects, demonstrating that both the presence of *Bt* and the production of Stx contribute to the morbidity and mortality during *C. rodentium* infection. It is noteworthy that the Δ*stx* DBS770 mutant behaves similarly to the WT DBS100 strain (which does not encode Stx) in the absence or presence of *Bt* (Figures S3 and 5). However, this effect is lost if *C. rodentium* is unable to form a functional T3SS and colonize (Figures 5A and 5B). The *cra* mutant, as expected, is also attenuated for infection (Figure S4), highlighting the importance of fluctuations of carbon metabolites during infection.

In *Bt*-reconstituted mice, *C. rodentium* virulence gene expression was increased compared to *C. rodentium* from microflora-deplete mice (Figures 5C and S5A). Analysis of the major phylogenetic groups determined that *Bacteroidetes* dominated the *Bt*-reconstituted groups on days 1 and 4 postinfection, while *Proteobacteria* dominated the microflora-deplete groups infected with *C. rodentium*. Maintenance of *Proteobacteria* was independent of Stx but dependent on a functional T3SS (Figure 5E). However, the bacterial burden of *C. rodentium* did not significantly differ in mice reconstituted with *Bt* and then challenged with *C. rodentium* compared to those not reconstituted with *Bt* (Figure S5B). Furthermore, examination of the ultrastructure of the distal colon showed destruction to the microvilli and attachment of *C. rodentium* to the epithelium (Figure 5D). The

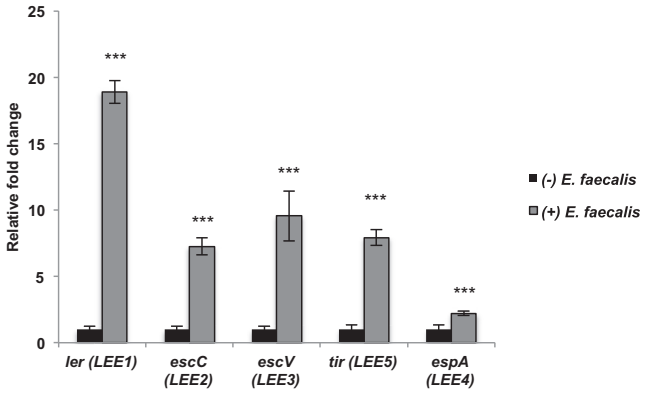

Figure 3. *E. faecalis*, a Member of the Firmicutes Phylum, Augments EHEC Virulence Gene Expression

qRT-PCR of LEE genes in EHEC grown alone (–) *E. faecalis* or in the presence of (+) *E. faecalis* (n = 9; error bars, SD; ***p < 0.001).

presence of *Bt* during *C. rodentium* infection does not cause a bloom in the *C. rodentium* population, but rather an increase in its virulence, akin to our observations in vitro (Figure 4).

Bt Contributes to the Accelerated Loss of a Protective Mucosal Layer during *C. rodentium* Infection

To determine if the increased morbidity and mortality that occurred during *C. rodentium* infection in *Bt*-reconstituted mice was due to increased host pathology, we evaluated the cecum and the colon for the following parameters: edema, crypt integrity, neutrophil infiltration, apoptosis, bacterial attachment, and vasculitis. The evaluation, performed in a double-blind fashion, demonstrated that host pathology was worsened in *Bt*-reconstituted mice, with augmented edema, vasculitis, apoptosis, and destruction of the crypts (Figure 6A, 6B, and S6). We also examined expression of host genes key in epithelial repair and in innate defense. Within the gastrointestinal tract, the mucus layer is the first line of defense against pathogens. The colon consists of two mucus layers—an outer layer that serves as a home to commensal bacteria and a tight inner layer devoid of bacteria (Johansson et al., 2013). In mice deficient in Muc2, the primary component of the colonic mucus layer, infection with *C. rodentium* causes rapid weight loss and mortality and increased gut permeability compared to WT mice (Bergstrom et al., 2010). Reconstitution with *Bt* during *C. rodentium* infection augmented the loss of Muc2 (Figure 6C). Transcription of intestinal trefoil factor 3 (*Tff3*), a secreted molecule important in epithelial repair and maintenance of the mucosa (Taupin and Podolsky, 2003), and Muc2 (*Muc2*) were significantly reduced during *C. rodentium* infection in *Bt*-reconstituted mice (*Tff3:* $p = 0.0283$; *Muc2:* $p = 0.0148$) (Figures 6D and 6E). Additionally, expression of the bacterial serine protease *p1411*, a homolog of Pic mucinase found in *Shigella* spp. and enteroaggregative *E. coli*, increased in *Bt*-reconstituted animals compared to mice deplete of microflora (Figure 6F). Consistent with the worsened damage to the crypts and mucosa, gut permeability increased in *Bt*-reconstituted mice during *C. rodentium* infection (Figure 6G). Host pathology is worsened during *C. rodentium* infection in *Bt*-reconstituted mice and likely contributes to the

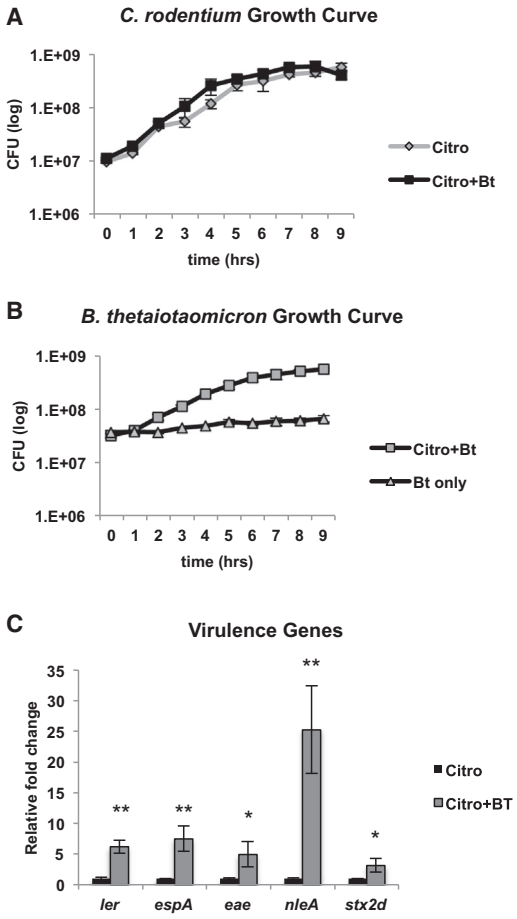

Figure 4. *C. rodentium* as an EHEC Infection Model

(A and B) Growth curves (of six biological samples, experiments were repeated two times, each with three independent biological samples) of in vitro growth of (A) *C. rodentium* or (B) *Bt*. The error bars indicate the SD of the mean. Doubling time for *C. rodentium* grown alone and in the presence of *Bt* is 69 min/gen and 66 min/gen, respectively. Doubling time for *Bt* grown alone and in the presence of *C. rodentium* is 282 min/gen and 91 min/gen, respectively.

(C) qRT-PCR of LEE, *nleA*, and *stx* genes in *C. rodentium* grown alone (–) *Bt* or in the presence of *Bt* (+) *Bt* (n = 6; error bars, SD; **p < 0.01, *p < 0.05).

increased morbidity and mortality in these mice. Conversely, transcription of the innate defense genes *Reg3*β and *Reg3*γ were increased during *C. rodentium* infection and augmented when *Bt* was also present (Figure S7). Of note, expression of RegIIIγ is increased in germ-free mice upon exposure to the microbiota, and this lectin kills only Gram-positive, but not Gram-negative, bacteria such as *Bt* and *C. rodentium* (Cash et al., 2006).

To further explore the mechanism of how *Bt* may be exerting its provirulence effect on *C. rodentium*, we examined metabolites present in the large intestine during infection. Our metabolomics studies showed that the metabolic landscape between mice colonized with *Bt* or not (PBS or *C. rodentium* infected animals) were quite diverse and that the *Bt* alone and *Bt* + *C. rodentium* animals have a more similar metabolite profile in their intestines (Figures 7A and 7B). Of note, several metabolites indicative of a gluconeogenic environment (such as lactate,

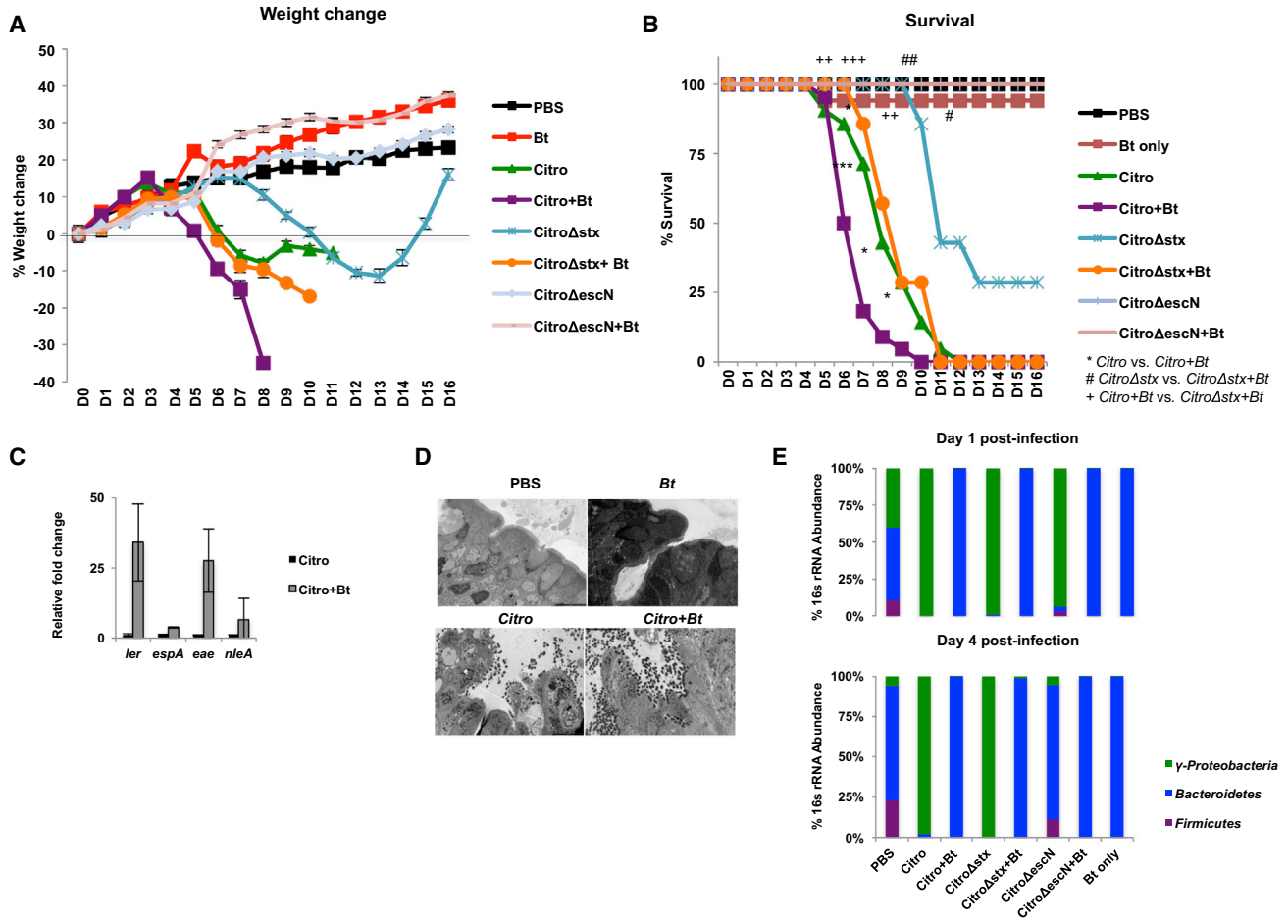

Figure 5. *Bt* Mediates Its Provirulence Effect on *C. rodentium* by Enhancing Expression of the T3SS, Not by a Bloom in the *C. rodentium* Population

C3H/HeJ mice were treated for 5 days with an antibiotics regimen to deplete gut microbiota. Half of the mice were reconstituted with *Bt* (+*Bt*) while the remainder of the mice were left deplete of gut microbiota. Mice were mock infected (PBS, *Bt* only) or infected with *C. rodentium* (*Citro*, Stx+), *C. rodentium*Δ*stx* (*Citro*Δ*stx*, Stx-), or *C. rodentium*Δ*escN* (*Citro*Δ*escN*).

(A) Weight loss or gain from baseline (weight at day 0) over the course of infection (blue: mock-infected, reconstituted with *Bt*; red: *Citro*-infected, deplete of microbiota; green: *Citro*-infected, reconstituted with *Bt*; purple: *Citro*Δ*stx*-infected, deplete of microbiota; turquoise: *Citro*Δ*stx*-infected, reconstituted with *Bt*; orange: *Citro*Δ*escN*-infected, deplete of microbiota; light blue: *Citro*Δ*escN*-infected, reconstituted with *Bt*).

(B) Survival after infection (n = 7–22 mice/group; error bars, SD; ***p < 0.001, **p < 0.01: comparison of *Citro* versus *Citro+Bt*; $^{\#\#}p < 0.01$, $^{\#}p < 0.05$: comparison of *Citro*Δ*stx* versus *Citro*Δ*stx+Bt*; $^{+++}p < 0.001$, $^{2+}p < 0.01$: comparison of *Citro+Bt* versus *Citro*Δ*stx+Bt*).

(C) qRT-PCR analysis of *ler*, *espA*, *eae*, and *nleA* from mRNA isolated from fecal pellets of infected animals. Significance is indicated as follows: *p ≰ 0.05, **p ≰ 0.01, and ***p ≰ 0.001.

(D) Ultrastructure of the distal colon harvested 5 days postinfection from mock-infected (PBS, *Bt*) or *C. rodentium*-infected mice either deplete of gut microbiota or reconstituted with *Bt*, 2,500×. Microvilli destruction and *C. rodentium* forming AE lesions on the colonic epithelium can be observed. Original magnification, 2,500× (TEM).

(E) qRT-PCR of 16 S rRNA from the major phylogenetic groups (green: *Proteobacteria*, blue: *Bacteroidetes*, and purple: *Firmicutes*) from feces collected on day 1 and day 4 postinfection.

succinate, glycerate, and others) were elevated in the *Bt*-treated animals (Figures 7A and 7B). Elevated concentrations of succinate, but not of fumarate or pyruvate, were measured within the cecum when *Bt* was present (Figure 7C), consistent with findings identifying succinate as a major metabolic by-product of *Bacteroides* spp (Macy et al., 1978). Succinate produced by *Bacteroides* spp. has been shown previously to impair neutrophil function and inhibit phagocytic killing of *E. coli* (Rotstein et al., 1985, 1989). Additionally, in a recent complementary study, Sonnenburg and colleagues demonstrated that microbiota-produced succinate induced after antibiotic treatment augments expansion of *C. difficile* in mice and that *C. difficile* deficient in succinate utilization pathways displayed a competitive disadvantage (Ferreyra et al., 2014). Moreover, the addition of succinate during in vitro culture of EHEC resulted in an increase in the expression of the LEE-encoded protein EspA in WT EHEC, wheras the *cra* mutant remains unresponsive to succinate (Figure 7D). It is also worth noting that *Enterococcus faecalis*, which

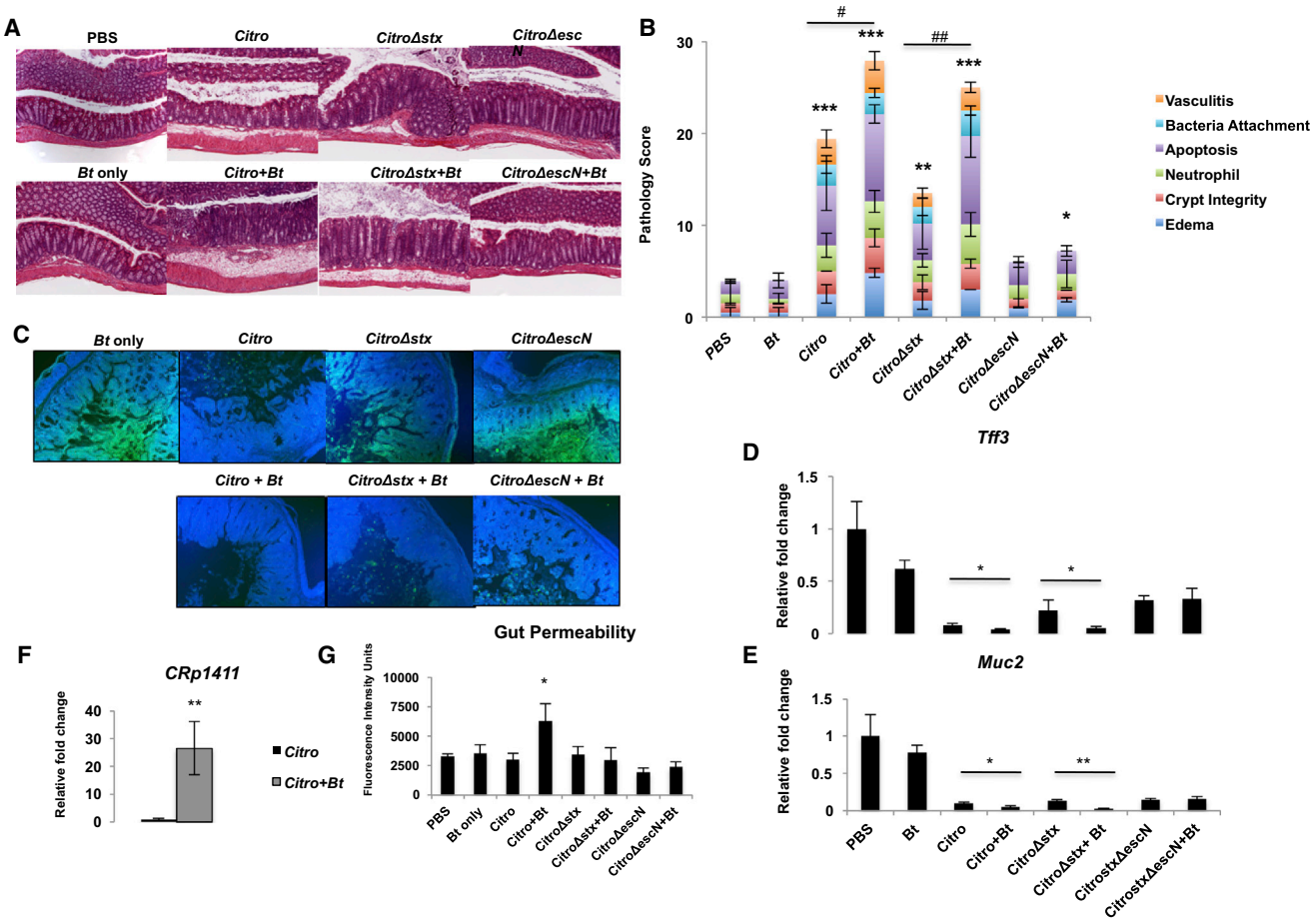

Figure 6. *Bt* Contributes to the Accelerated Loss of a Protective Mucosal Layer during *C. rodentium* Infection

(A and B) Antibiotics-treated C3H/HeJ mice either deplete of gut microbiota or reconstituted with *Bt* (+*Bt*) were mock-infected (PBS, *Bt* only) or infected with *C. rodentium* (*Citro*, Stx+), *C. rodentium*Δ*stx* (*Citro*Δ*stx*, Stx-), or *C. rodentium*Δ*escN* (*Citro*Δ*escN*). The histological changes in the colon and cecum were analyzed on day 5 postinfection based on the following scoring system: edema, 0 is no edema and 5 has the highest edema in the submucosa; crypt integrity, 1 = normal, 2 = irregular crypts, 3 = mild crypt loss, 4 = severe crypt loss, and 5 = complete crypt loss; neutrophil, neutrophilic infiltration in the wall; apoptosis, number of apoptotic cells per 600× field (n = five fields); bacteria attachment, bacteria associated to the epithelial surface; vasculitis, 0 is no evidence of vasculitis and 5 is the most severe vasculitis. Scoring was performed blindly, and the scores for each parameter are an average of the cecum and distal colon, taken from two independent experiments with three mice/experiment.

(C) Cecum harvested on day 5 postinfection was stained with Muc2 (green) and DAPI (DNA, blue). Original magnification, 10×.

(D and E) qRTPCR of (D) *Tff3* and (E) *Muc2*. RNA was isolated from colonic tissue harvested from mice on day 5 postinfection. (n = 6; error bars, SD).

(F) qRT-PCR of *p1411* from feces collected on day 2 postinfection.

(G) Levels of FITC-Dextran in the serum of mice on day 5 postinfection. Mice were fasted 4 hr prior to administration of FITC-Dextran via oral gavage. FITC-Dextran levels were determined by measuring fluorescence at excitation 490 nm, emission 525 nm (n = 6; error bars, SD; ***p < 0.001, **p < 0.01, *p < 0.05, p > 0.05 = ns).

also increases EHEC virulence gene expression (Figure 3), also produces and secretes copious amounts of succinate (Milstien and Goldman, 1973).

Interestingly, *Bt* colonization increases the levels of γ-L- glutamyl-L-cysteinyl-glycine, or glutathione (GSH), and its precursors cysteine and S-adenosyl-homocysteine (Figure 7A). GSH plays a role in nutrient metabolism, antioxidant defense, and a number of key cellular metabolic functions (Aquilano et al., 2014). Additionally, *Bt* colonization alone increases the gluconeogenic metabolites succinate, glycerate, and lactate, creating a different metabolic landscape for *C. rodentium* than what the pathogen encounters in the microflora-deplete animals. In the *C. rodentium*-infected animals deplete of a microflora, the levels of nucleosides (cytidine, guanosine, thymidine, and uridine) are decreased compared to mock-infected animals. The presence of *Bt* in *C. rodentium*-infected animals rescues this decrease in nucleosides and nucleic acid precursors (Figure 7A). Our findings begin to delve into the specific metabolites that a key constituent of the microbiota, *Bt*, contributes to the intestinal environment, and we link this metabolic environment to an increase in virulence of an enteric pathogen.

DISCUSSION

The interaction between a host and its gastrointestinal microflora is a delicate balance and if disturbed can result in dysbiosis (Spor

A

Metabolite	Bt/PBS	Citro/PBS	Citro+Bt/ PBS	Citro+Bt/ Citro	Citro+Bt/ Bt
2-hydroxyglutaric acid	38.66	0.90	229.60	256.23	5.94
CMP	1.07	1.08	3.65	3.39	3.40
cytidine	0.65	0.06	0.40	6.16	0.61
gluconic acid	0.66	0.22	0.09	0.41	0.14
guanosine	0.42	0.08	0.26	3.09	0.62
2-deoxycytidine	0.73	0.05	0.27	5.96	0.37
2-isopropylmalic acid	1.42	2.44	0.66	0.27	0.46
2-ketohaxonic acid	7.89	1.47	4.71	3.21	0.60
3-hydroxybutyrate	2.12	1.13	2.36	2.09	1.11
7-methylguanosine	5.14	0.87	3.29	3.76	0.64
adenosine	5.18	1.86	5.62	3.02	1.09
ascorbic acid	1.35	2.38	0.63	0.26	0.47
cadaverine	1.72	5.73	9.39	1.64	5.47
carnitine-C3	3.18	0.96	8.85	9.19	2.78
cysteine	282.13	155.28	565.61	3.64	2.00
dAMP	0.80	0.80	5.29	6.63	6.58
deoxyinosine	0.51	0.03	0.15	4.93	0.30
deoxyuridine	0.36	0.00	0.10	58.50	0.29
flavin adenine dinucleotide	3.13	1.30	3.55	2.72	1.13
glucarate	0.79	0.25	0.61	2.40	0.77
glutamate/NMDA	2.05	2.29	5.15	2.25	2.51
glycerate	48.54	0.90	72.39	80.78	1.49
glycerophosphorylcholine	1.29	0.22	0.14	0.62	0.10
glycine	0.71	2.56	2.44	0.95	3.42
GSH	82.25	0.90	3463.48	3865.10	42.11
guanine	0.60	0.13	0.37	2.97	0.62
hydroxyisocaproic acid	7232.29	1906.05	1989.32	1.04	0.28
kynurenine	0.84	1.21	3.34	2.76	3.98
malic acid	6.44	3.84	11.93	3.10	1.85
NAD	8.51	2.77	22.03	7.96	2.59
nicotinamide	0.50	0.54	1.43	2.66	2.86
ornithine	8.12	7.25	5.93	0.82	0.73
pantothenic acid	2.15	1.80	3.84	2.13	1.78
phenyl-lactic acid	236.01	139.47	401.03	2.88	1.70
S-adenosyl-homocysteine	131.79	0.90	90.79	101.32	0.69
succinate/methyl-malonic acid	200.57	37.06	201.05	5.43	1.00
thiamine	0.37	1.07	0.07	0.07	0.20
thymidine	0.57	0.03	0.23	6.59	0.39
UDP	1.04	5.52	15.91	2.88	15.26
uridine	0.58	0.15	0.45	3.10	0.79

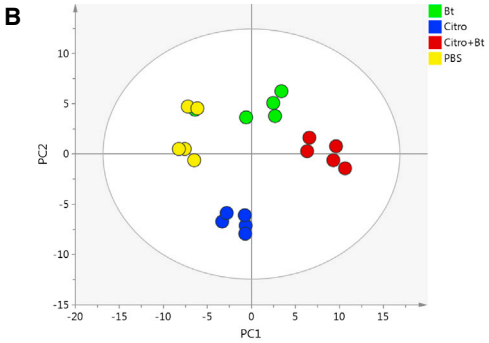

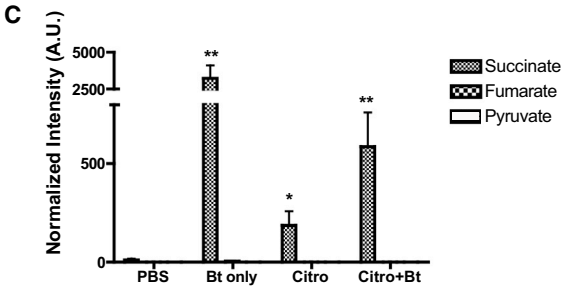

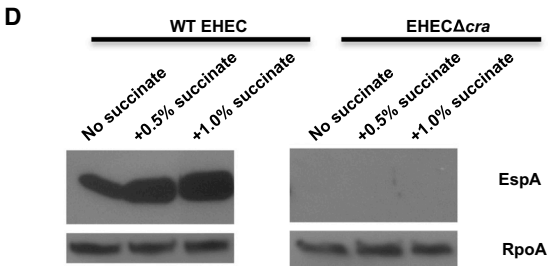

Figure 7. Comparison of Metabolic Profiles of *Bt*-Reconstituted and Microflora-Deplete Animals

(A) The expression profiling of metabolites present in the cecum on day 2 postinfection (n = 5). The data are presented as ratios to show fold-changes of the specified metabolite in the individual groups.

(B) The normalized data were analyzed by principal component analysis (PCA) with unit variance scaling in order to obtain an unbiased overview of the data and to visualize clustering, trends, and outlier metabolites among all groups on the score plots. PCA score plots showed clear separation among the four groups in different colors (yellow: PBS, red: Citro+Bt, blue: Citro, green: Bt) with no outliers detected. The amount of variance in the *X* matrix explained by PC1 (R^2) was 0.732, and estimate of the predictive ability of the model (Q^2) (cumulative) was 0.446.

(C) Absolute levels of succinate, fumarate, and pyruvate present in the cecum on day 2 postinfection. (A.U. Absolute Units; n = 5; error bars, SD; $^{**}p < 0.01$, $^{*}p < 0.05$).

(D) Protein level of the T3SS translocon protein EspA, encoded within *LEE4*, secreted into the supernatant of WT or Δ*cra* EHEC cultures grown in the presence of 0.1% glucose, plus increasing levels of succinate. RpoA protein levels in the cell lysate serve as the loading control.

et al., 2011). Host balance with the microbiota is maintained in part through the C-type lectins RegIIIβ and RegIIIγ that limit direct interaction of the microbiota with the intestinal microbiota (Cash et al., 2006; Vaishnava et al., 2011) and in part through maintenance of the integrity of the intestinal epithelium. Intestinal TFF3 secreted by goblet cells plays an essential role in epithelial repair and restoration of the mucosa (Taupin and Podolsky, 2003). Some pathogens, however, evade these host defenses and can even benefit from them. *Salmonella typhimurium* thrives in an inflammatory environment due to the production of RegIIIβ that eliminates competing microbiota (Stelter et al., 2011). In hosts with a high-fiber diet, butyrate—a beneficial metabolite in colonic health—enhances the expression of the Stx receptor globotriaosylceramide (Gb3) and increases susceptibility to EHEC O157:H7 infection (Zumbrun et al., 2013). Our studies indicate that a normally beneficial member of the microbiota has the capacity to enhance virulence and disease progression of an enteric pathogen, altering the metabolic landscape toward a gluconeogenic environment and secreting large amounts of the succinate metabolite within the intestine that is interpreted by the pathogen, through the transcription factor Cra as a nutritional cue to activate virulence gene expression. Recent findings corroborate the idea that the microbiota can provide a competitive advantage to enteric pathogens (Ng et al., 2013). Our findings

have fundamental implications into how the composition of the microbiota impacts pathogen-mediated disease susceptibility and progression and show that certain enteric pathogens learned to exploit the microbiota to enhance their virulence.

EXPERIMENTAL PROCEDURES

Strains and Culture Conditions

Strains used in this study are listed in Table S1. *B. thetaiotaomicron* VPI-5482 was grown anaerobically overnight at 37°C in TYG medium (Betian et al., 1977) plus 200 μg/ml gentamicin. WT EHEC O157:H7 strain 86-24 (Griffin et al., 1988) and its isogenic mutants (*ΔqseC*, *ΔqseE*, *Δcra*, *ΔkdpE*, *ΔcraΔkdpE*, and *ΔfusK*) were grown anaerobically overnight at 37°C in LB plus 50 μg/ml streptomycin. *C. rodentium* strains DBS770 ($\lambda stx_{2\ dact}$) and its isogenic mutant MMC01 (CRΔ*escN*) were grown anaerobically overnight in LB plus 25 μg/ml chloramphenicol. The lysogenized, Stx-deficient *C. rodentium* strain DBS771 was grown in LB plus 50 μg/ml kanamycin (Mallick et al., 2012). *Bt* overnight culture was pelleted and concentrated 10-fold in LB. *Bt* was plated in a 10-fold excess over EHEC or *C. rodentium* to represent the composition of the intestinal microbiota. *E. faecalis* V583 (Paulsen et al., 2003) was grown anaerobically in LB overnight, and the overnight culture was plated at a 1:1 with EHEC. The bacteria were grown anaerobically in Petri dishes in 25 ml of prereduced low-glucose Dulbecco's modified Eagle's medium (DMEM) (Invitrogen) for 6 hr, unless otherwise noted, in a GasPak EZ anaerobe container (Becton Dickinson). RNA was extracted using a RiboPure Bacteria RNA isolation kit (Ambion) according to manufacturer's guidelines.

Microarray Preparation and Analyses

Affymetrix 2.0 *E. coli* gene arrays were used to compare gene expression in strain 86-24 when cultured alone to that in strain 86-24 when grown in the presence of *Bt*, grown anaerobically in prereduced DMEM at 37°C for 6 hr to late-log phase in a GasPak EZ anaerobe container. The relative abundance of EHEC to *Bt* at the time of RNA harvest was 70% EHEC and 30% *Bt*. *Bt* grown alone was included as a control to ensure that *Bt* cDNA did not hybridize to the *E. coli* gene array. The RNA processing, labeling, hybridization, and slide-scanning procedures were performed as described in the Affymetrix Gene Expression technical manual. The array data analyses were performed as described previously (Kendall et al., 2011). Based on array data analyses, the biological processes of the genes significantly increased ≥4-fold (406 genes, 297 with known functions and 109 with unknown function) or significantly decreased ≥2-fold (72 genes, 58 with known functions and 14 with unknown function) were characterized using the Universal Protein Resource (UniProt) Knowledgebase (UniProtKB/Swiss-Prot) (http://www.uniprot.org).

Growth Curves

Bacteria were cultured as described above for 9 hr. Bacteria were serially diluted in PBS each hour and then plated on the following agar plates: LB agar plus 50 μg/ml streptomycin (isolation of EHEC O157:H7), LB agar plus 25 μg/ml chloramphenicol (isolation of *C. rodentium*), or Brain Heart Infusion (BHI) agar (VWR) plus 10% calf blood (Colorado Serum Company) plus 200 μg/ml gentamicin (isolation of *Bt*). EHEC O157:H7 and *C. rodentium* plates were grown aerobically at 37°C for 24 hr. *Bt* plates were grown anaerobically at 37°C for 48 hr. In each experiment, bacteria were grown on both selection plates to confirm that growth was selective. To determine the growth rate, two points from the exponential phase were selected (t = 2 hr, t = 5 hr) and calculated using the formula: $k = \log_{10}[X_t] - \log_{10}[X_0]$, where X_t = higher cfu/ml, X_0 = lower cfu/ml, and 0.301 × t = time interval (in hours) between the points. Generation time was then calculated as $t_{gen} = 1/k$.

Real-Time qPCR

For in vitro experiments, cultures were grown to late-log phase in prereduced DMEM under anaerobic conditions (6 hr). For in vivo experiments, fecal pellets were collected from infected mice on days 0, 1, and 4 after *C. rodentium* infection. RNA was extracted using the RiboPure Bacteria isolation kit according to the manufacturer's protocols (Ambion). To assess host gene expression, tissue from the distal colon of infected mice was harvested on day 5 postinfection and homogenized in 1 ml TRIzol (Life Technologies) per 100 mg tissue. RNA was isolated using standard molecular biological procedures. The primers used for quantitative reverse transcription-PCR (qRT-PCR) (Table S2) were validated for amplification efficiency and template specificity. qRT-PCR was performed as previously described (Hughes et al., 2009) in a one-step reaction using an ABI 7500 sequence detection system (Applied Biosystems). Data were collected using the ABI Sequence Detection 1.2 software (Applied Biosystems).

All data were normalized to an endogenous control (*rpoA* for virulence gene expression in EHEC and *C. rodentium*, *Eubacteria* 16S rRNA for total bacteria present in feces, or *GAPDH* for murine host gene expression in colonic tissue) and analyzed using the comparative critical threshold (C_T) method. Virulence gene expression was presented as fold changes over the expression level of WT EHEC or *C. rodentium* cultured alone in vitro or *C. rodentium* (DBS770) infected alone in vivo. Host gene expression was presented as fold changes over the expression level present in mock-infected (PBS) mice.

The relative abundances of *Bacteroidetes*, *Firmicutes*, *and Proteobacteria* (family *Enterobacteriaceae*) were measured by qPCR with taxon-specific or universal 16S rRNA gene primers. The primers used were as follows: Eubacteria (universal bacteria), Eub338F, 5′- actcctacgggaggcagcagt-3′, and Eub338R, 5′- attaccgcggctgctggc-3′; Firmicutes, 928F-Firm, 5′-tgaaactyaaaggaattg acg-3′, and 1040FirmR, 5′-accatgcaccacctgtc-3′ (Bacchetti De Gregoris et al., 2011); Bacteroidetes, 798cfbF, 5′- craacaggattagataccct-3′, and cfb 967R, 5′- ggtaaggttcctcgcgtat-3′ (Guo et al., 2008); and γ-Proteobacteria, 1080 gF, 5′- tcgtcagctcgtgtygtga-3′, and g1202R, 5′- cgtaagggccatgatg-3′ (Bacchetti De Gregoris et al., 2011). Expression of each taxon was normalized to Eub388 and then compared to the expression level present in mock-infected (PBS) fecal pellets on day 0 (D0). Percentage of taxa was determined by dividing the expression of the taxon-specific 16S rRNA over the combined expression of *Firmicutes*, *Bacteroidetes*, *and γ-Proteobacteria*. The Student's unpaired t test was used to determine statistical significance.

Fluorescein Actin Staining

Fluorescein actin staining assays were performed as described by Knutton et al. (1989). Briefly, HeLa cells were grown on coverslips in 12-well culture plates with DMEM supplemented with 10% fetal bovine serum (FBS) and 1% penicillin/streptomycin/gentamicin antibiotic mix at 37°C, 5% CO_2, overnight to 80% confluency. The wells were washed with PBS and replaced with low-glucose DMEM supplemented with 10% FBS. Bacterial cultures were grown anaerobically overnight as described above at 37°C, and overnight *Bt* culture was concentrated 10-fold in LB. Overnight bacterial cultures were diluted 1:100 to infect confluent monolayers of HeLa cells for 6 hr at 37°C, 5% CO_2. After a 6 hr infection, the coverslips were washed, fixed, permeabilized, and treated with fluorescein isothiocyanate (FITC)-labeled phalloidin to visualize actin accumulation and propidium iodide to visualize host nuclei and bacteria. The coverslips were mounted on slides and visualized with a Zeiss Axiovert microscope. To determine percentage infected cells, five to seven fields from three separate coverslips (triplicate) were counted and calculated as (Cells with Pedestals/Total cells)•100. Statistical analyses were performed using the Student's unpaired t test.

Mice

C3H/HeJ mice were purchased from The Jackson Laboratory and housed in a specific pathogen-free facility at UT Southwestern Medical Center. All experiments were performed under IACUC approved protocols.

At 3 to 4 weeks of age, female C3H/HeJ mice were orally administered a combination of four antibiotics: ampicillin, neomycin, metronidazole, and vancomycin (Sigma-Aldrich) via oral gavage for 5 or 6 days to deplete gut microbiota (5 mg of each antibiotic per mouse per day) (Rakoff-Nahoum et al., 2004). Fecal pellets were collected before and after antibiotics treatment to confirm depletion of the gut microbiota. Feces were resuspended in PBS at 1 g/ml, serially diluted, and plated on BHI-Blood agar plates containing no antibiotics. Colony counts were performed after 48 hr incubation at 37°C under both aerobic and anaerobic conditions. Following antibiotics treatment, half of the mice were reconstituted with 3 × 10^9 colony-forming units (cfu) *Bt* via oral gavage while the remainder of the mice were left deplete of gut microbiota. Twenty hours later, mice were mock infected with PBS or orally infected with 1 × 10^9 cfu *C. rodentium* (DBS770, Stx+), *C. rodentiumΔstx* (DBS771, Stx-), *C. rodentiumΔescN* (MMC01, *CitroΔescN*), or *C. rodentiumΔcra* (MMC02, *CitroΔcra*).

Baseline weight of mice was measured on the initial day of *C. rodentium* infection (D0). Mice were weighed daily for the course of infection. Percentage weight was calculated in the following way: [(Weight$_{Day\ n}$ – Baseline weight)/Baseline weight]•100. Change in weight reflects weight gain or weight loss over the course of infection. Mice were monitored daily for survival. The experiments were performed at least twice with a total of 7–22 mice per group. Weight change and survival curves reflect the average of experiments plus the SD. The Student's unpaired t test was used to determine the statistical significance of each day on the survival curve.

To measure gut permeability, mice were fasted for 4 hr prior to administration of 20 ml/kg of FITC-dextran (Sigma) via oral gavage on day 5 postinfection with *C. rodentium*. Fasting conditions were maintained for an additional 3 hr, at which point blood was collected and centrifuged to collect plasma. Serum was diluted 1:2 in PBS and fluorescence at excitation 490 nm, emission 520 nm, was measured using a fluorimeter. A standard curve was prepared by serially diluting FITC-dextran in a consistent PBS:mouse serum with the samples.

Histopathology

Portions of the distal colon and cecum were harvested 5 days postinfection with *C. rodentium*. The tissues were washed in PBS and then fixed in Bouin's fixative for 48 hr. The tissues were embedded in paraffin, cut into 5-μm sections, and stained with hematoxylin and eosin in the UT Southwestern Pathology Core. Histological changes were analyzed in a double-blind fashion. The severity of intestinal pathology was analyzed based on the following scoring system: edema, 0 is no edema and 5 has the highest edema in the submucosa; crypt integrity, 1 = normal, 2 = irregular crypts, 3 = mild crypt loss, 4 = severe crypt loss, and 5 = complete crypt loss; neutrophil, neutrophilic infiltration in the wall; apoptosis, number of apoptotic cells per 600 × field (n = five fields); bacteria attachment, bacteria associated to the epithelial surface; goblet cell, average number of goblet cell in each crypt (n > 10 crypts); and vasculitis, 0 is no evidence of vasculitis and 5 is the most severe vasculitis. The scores for each parameter are an average of the cecum and distal colon, taken from two independent experiments with three mice/experiment.

ACCESSION NUMBERS

Microarray data are deposited in the Gene Expression Omnibus under accession number GSE47418.

SUPPLEMENTAL INFORMATION

Supplemental Information includes seven figures, three tables, and Supplemental Experimental Procedures and can be found with this article online at http://dx.doi.org/10.1016/j.chom.2014.11.005.

AUTHOR CONTRIBUTIONS

M.M.C. led the project, performed and designed experiments, and wrote the paper. Z.H., C.K., and R.J.D. performed the metabolomics experiments. S.N. performed the double-blind histopathology analysis. V.S. designed experiments and wrote the paper.

ACKNOWLEDGMENTS

Thank you to the Microarray Core, the Pathology Core, and the Electron Microscopy Core at UT Southwestern for their help in processing samples. This work was supported by the National Institute of Health (NIH) Grants AI053067, AI77853, and AI077613 and the Burroughs Wellcome Fund (V.S.). M.M.C. was supported through NIH Training Grant 5 T32 AI7520-14. The contents are solely the responsibility of the authors and do not represent the official views of the NIH NIAID.

Received: August 20, 2014
Revised: September 26, 2014
Accepted: November 6, 2014
Published: December 10, 2014

REFERENCES

Aquilano, K., Baldelli, S., and Ciriolo, M.R. (2014). Glutathione: new roles in redox signaling for an old antioxidant. Front. Pharmacol. *5*, 196.

Bacchetti De Gregoris, T., Aldred, N., Clare, A.S., and Burgess, J.G. (2011). Improvement of phylum- and class-specific primers for real-time PCR quantification of bacterial taxa. J. Microbiol. Methods *86*, 351–356.

Bergstrom, K.S., Kissoon-Singh, V., Gibson, D.L., Ma, C., Montero, M., Sham, H.P., Ryz, N., Huang, T., Velcich, A., Finlay, B.B., et al. (2010). Muc2 protects against lethal infectious colitis by disassociating pathogenic and commensal bacteria from the colonic mucosa. PLoS Pathog. *6*, e1000902.

Betian, H.G., Linehan, B.A., Bryant, M.P., and Holdeman, L.V. (1977). Isolation of a cellulotytic Bacteroides sp. from human feces. Appl. Environ. Microbiol. *33*, 1009–1010.

Borody, T.J., and Khoruts, A. (2012). Fecal microbiota transplantation and emerging applications. Nat. Rev. Gastroenterol. Hepatol. *9*, 88–96.

Cash, H.L., Whitham, C.V., Behrendt, C.L., and Hooper, L.V. (2006). Symbiotic bacteria direct expression of an intestinal bactericidal lectin. Science *313*, 1126–1130.

Chin, A.M., Feldheim, D.A., and Saier, M.H., Jr. (1989). Altered transcriptional patterns affecting several metabolic pathways in strains of Salmonella typhimurium which overexpress the fructose regulon. J. Bacteriol. *171*, 2424–2434.

Dicksved, J., Ellstrom, P., Engstrand, L., and Rautelin, H. (2014). Susceptibility to campylobacter infection is associated with the species composition of the human fecal microbiota. MBio. *5*, e01212–e01214.

Feldheim, D.A., Chin, A.M., Nierva, C.T., Feucht, B.U., Cao, Y.W., Xu, Y.F., Sutrina, S.L., and Saier, M.H., Jr. (1990). Physiological consequences of the complete loss of phosphoryl-transfer proteins HPr and FPr of the phosphoenolpyruvate:sugar phosphotransferase system and analysis of fructose (fru) operon expression in Salmonella typhimurium. J. Bacteriol. *172*, 5459–5469.

Ferreyra, J.A., Wu, K.J., Hryckowian, A.J., Bouley, D.M., Weimer, B.C., and Sonnenburg, J.L. (2014). Gut microbiota-produced succinate promotes *C. difficile* infection after antibiotic treatment or motility disturbance. Cell Host Microbe *16*, this issue, 770–777.

Gevers, D., Kugathasan, S., Denson, L.A., Vázquez-Baeza, Y., Van Treuren, W., Ren, B., Schwager, E., Knights, D., Song, S.J., Yassour, M., et al. (2014). The treatment-naive microbiome in new-onset Crohn's disease. Cell Host Microbe *15*, 382–392.

Griffin, P.M., Ostroff, S.M., Tauxe, R.V., Greene, K.D., Wells, J.G., Lewis, J.H., and Blake, P.A. (1988). Illnesses associated with Escherichia coli O157:H7 infections. A broad clinical spectrum. Ann. Intern. Med. *109*, 705–712.

Guo, X., Xia, X., Tang, R., Zhou, J., Zhao, H., and Wang, K. (2008). Development of a real-time PCR method for Firmicutes and Bacteroidetes in faeces and its application to quantify intestinal population of obese and lean pigs. Lett. Appl. Microbiol. *47*, 367–373.

Honda, K., and Littman, D.R. (2012). The microbiome in infectious disease and inflammation. Annu. Rev. Immunol. *30*, 759–795.

Hooper, L.V., Midtvedt, T., and Gordon, J.I. (2002). How host-microbial interactions shape the nutrient environment of the mammalian intestine. Annu. Rev. Nutr. *22*, 283–307.

Hughes, D.T., Clarke, M.B., Yamamoto, K., Rasko, D.A., and Sperandio, V. (2009). The QseC adrenergic signaling cascade in Enterohemorrhagic E. coli (EHEC). PLoS Pathog. *5*, e1000553.

Johansson, M.E., Sjövall, H., and Hansson, G.C. (2013). The gastrointestinal mucus system in health and disease. Nat. Rev. Gastroenterol. Hepatol. *10*, 352–361.

Kaper, J.B., Nataro, J.P., and Mobley, H.L. (2004). Pathogenic Escherichia coli. Nat. Rev. Microbiol. *2*, 123–140.

Kelly, C.R., Ihunnah, C., Fischer, M., Khoruts, A., Surawicz, C., Afzali, A., Aroniadis, O., Barto, A., Borody, T., Giovanelli, A., et al. (2014). Fecal microbiota transplant for treatment of Clostridium difficile infection in immunocompromised patients. Am. J. Gastroenterol. *109*, 1065–1071.

Kendall, M.M., Gruber, C.C., Rasko, D.A., Hughes, D.T., and Sperandio, V. (2011). Hfq virulence regulation in enterohemorrhagic Escherichia coli O157:H7 strain 86-24. J. Bacteriol. *193*, 6843–6851.

Knutton, S., Baldwin, T., Williams, P.H., and McNeish, A.S. (1989). Actin accumulation at sites of bacterial adhesion to tissue culture cells: basis of a new diagnostic test for enteropathogenic and enterohemorrhagic Escherichia coli. Infect. Immun. *57*, 1290–1298.

Kuss, S.K., Best, G.T., Etheredge, C.A., Pruijssers, A.J., Frierson, J.M., Hooper, L.V., Dermody, T.S., and Pfeiffer, J.K. (2011). Intestinal microbiota promote enteric virus replication and systemic pathogenesis. Science *334*, 249–252.

Larsen, N., Vogensen, F.K., van den Berg, F.W., Nielsen, D.S., Andreasen, A.S., Pedersen, B.K., Al-Soud, W.A., Sørensen, S.J., Hansen, L.H., and Jakobsen, M. (2010). Gut microbiota in human adults with type 2 diabetes differs from non-diabetic adults. PLoS ONE *5*, e9085.

Macy, J.M., Ljungdahl, L.G., and Gottschalk, G. (1978). Pathway of succinate and propionate formation in Bacteroides fragilis. J. Bacteriol. *134*, 84–91.

Mallick, E.M., McBee, M.E., Vanguri, V.K., Melton-Celsa, A.R., Schlieper, K., Karalius, B.J., O'Brien, A.D., Butterton, J.R., Leong, J.M., and Schauer, D.B. (2012). A novel murine infection model for Shiga toxin-producing Escherichia coli. J. Clin. Invest. *122*, 4012–4024.

Milstien, S., and Goldman, P. (1973). Role of intestinal microflora in the metabolism of guanidinosuccinic acid. J. Bacteriol. *114*, 641–644.

Mundy, R., MacDonald, T.T., Dougan, G., Frankel, G., and Wiles, S. (2005). Citrobacter rodentium of mice and man. Cell. Microbiol. *7*, 1697–1706.

Ng, K.M., Ferreyra, J.A., Higginbottom, S.K., Lynch, J.B., Kashyap, P.C., Gopinath, S., Naidu, N., Choudhury, B., Weimer, B.C., Monack, D.M., and Sonnenburg, J.L. (2013). Microbiota-liberated host sugars facilitate post-antibiotic expansion of enteric pathogens. Nature *502*, 96–99.

Njoroge, J., and Sperandio, V. (2012). Enterohemorrhagic Escherichia coli virulence regulation by two bacterial adrenergic kinases, QseC and QseE. Infect. Immun. *80*, 688–703.

Njoroge, J.W., Nguyen, Y., Curtis, M.M., Moreira, C.G., and Sperandio, V. (2012). Virulence meets metabolism: Cra and KdpE gene regulation in enterohemorrhagic Escherichia coli. MBio *3*, e00280–e12.

Njoroge, J.W., Gruber, C., and Sperandio, V. (2013). The interacting Cra and KdpE regulators are involved in the expression of multiple virulence factors in enterohemorrhagic Escherichia coli. J. Bacteriol. *195*, 2499–2508.

Pacheco, A.R., Curtis, M.M., Ritchie, J.M., Munera, D., Waldor, M.K., Moreira, C.G., and Sperandio, V. (2012). Fucose sensing regulates bacterial intestinal colonization. Nature *492*, 113–117.

Paulsen, I.T., Banerjei, L., Myers, G.S., Nelson, K.E., Seshadri, R., Read, T.D., Fouts, D.E., Eisen, J.A., Gill, S.R., Heidelberg, J.F., et al. (2003). Role of mobile DNA in the evolution of vancomycin-resistant Enterococcus faecalis. Science *299*, 2071–2074.

Peterson, D.A., Frank, D.N., Pace, N.R., and Gordon, J.I. (2008). Metagenomic approaches for defining the pathogenesis of inflammatory bowel diseases. Cell Host Microbe *3*, 417–427.

Rakoff-Nahoum, S., Paglino, J., Eslami-Varzaneh, F., Edberg, S., and Medzhitov, R. (2004). Recognition of commensal microflora by toll-like receptors is required for intestinal homeostasis. Cell *118*, 229–241.

Reading, N.C., Torres, A.G., Kendall, M.M., Hughes, D.T., Yamamoto, K., and Sperandio, V. (2007). A novel two-component signaling system that activates transcription of an enterohemorrhagic Escherichia coli effector involved in remodeling of host actin. J. Bacteriol. *189*, 2468–2476.

Rotstein, O.D., Pruett, T.L., Fiegel, V.D., Nelson, R.D., and Simmons, R.L. (1985). Succinic acid, a metabolic by-product of Bacteroides species, inhibits polymorphonuclear leukocyte function. Infect. Immun. *48*, 402–408.

Rotstein, O.D., Vittorini, T., Kao, J., McBurney, M.I., Nasmith, P.E., and Grinstein, S. (1989). A soluble Bacteroides by-product impairs phagocytic killing of Escherichia coli by neutrophils. Infect. Immun. *57*, 745–753.

Saier, M.H., Jr., and Ramseier, T.M. (1996). The catabolite repressor/activator (Cra) protein of enteric bacteria. J. Bacteriol. *178*, 3411–3417.

Sommer, F., and Bäckhed, F. (2013). The gut microbiota—masters of host development and physiology. Nat. Rev. Microbiol. *11*, 227–238.

Sonnenburg, J.L., Xu, J., Leip, D.D., Chen, C.H., Westover, B.P., Weatherford, J., Buhler, J.D., and Gordon, J.I. (2005). Glycan foraging in vivo by an intestine-adapted bacterial symbiont. Science *307*, 1955–1959.

Sperandio, V., Torres, A.G., and Kaper, J.B. (2002). Quorum sensing Escherichia coli regulators B and C (QseBC): a novel two-component regulatory system involved in the regulation of flagella and motility by quorum sensing in E. coli. Mol. Microbiol. *43*, 809–821.

Spor, A., Koren, O., and Ley, R. (2011). Unravelling the effects of the environment and host genotype on the gut microbiome. Nat. Rev. Microbiol. *9*, 279–290.

Stelter, C., Käppeli, R., König, C., Krah, A., Hardt, W.D., Stecher, B., and Bumann, D. (2011). Salmonella-induced mucosal lectin RegIIIβ kills competing gut microbiota. PLoS ONE *6*, e20749.

Taupin, D., and Podolsky, D.K. (2003). Trefoil factors: initiators of mucosal healing. Nat. Rev. Mol. Cell Biol. *4*, 721–732.

Turnbaugh, P.J., Hamady, M., Yatsunenko, T., Cantarel, B.L., Duncan, A., Ley, R.E., Sogin, M.L., Jones, W.J., Roe, B.A., Affourtit, J.P., et al. (2009a). A core gut microbiome in obese and lean twins. Nature *457*, 480–484.

Turnbaugh, P.J., Ridaura, V.K., Faith, J.J., Rey, F.E., Knight, R., and Gordon, J.I. (2009b). The effect of diet on the human gut microbiome: a metagenomic analysis in humanized gnotobiotic mice. Sci. Transl. Med. *1*, 6ra14.

Vaishnava, S., Yamamoto, M., Severson, K.M., Ruhn, K.A., Yu, X., Koren, O., Ley, R., Wakeland, E.K., and Hooper, L.V. (2011). The antibacterial lectin RegIIIgamma promotes the spatial segregation of microbiota and host in the intestine. Science *334*, 255–258.

Walter, J., and Ley, R. (2011). The human gut microbiome: ecology and recent evolutionary changes. Annu. Rev. Microbiol. *65*, 411–429.

Wang, Y., Hoenig, J.D., Malin, K.J., Qamar, S., Petrof, E.O., Sun, J., Antonopoulos, D.A., Chang, E.B., and Claud, E.C. (2009). 16S rRNA gene-based analysis of fecal microbiota from preterm infants with and without necrotizing enterocolitis. ISME J. *3*, 944–954.

Willing, B.P., Vacharaksa, A., Croxen, M., Thanachayanont, T., and Finlay, B.B. (2011). Altering host resistance to infections through microbial transplantation. PLoS ONE *6*, e26988.

Xu, J., Bjursell, M.K., Himrod, J., Deng, S., Carmichael, L.K., Chiang, H.C., Hooper, L.V., and Gordon, J.I. (2003). A genomic view of the human-Bacteroides thetaiotaomicron symbiosis. Science *299*, 2074–2076.

Zumbrun, S.D., Melton-Celsa, A.R., Smith, M.A., Gilbreath, J.J., Merrell, D.S., and O'Brien, A.D. (2013). Dietary choice affects Shiga toxin-producing Escherichia coli (STEC) O157:H7 colonization and disease. Proc. Natl. Acad. Sci. USA *110*, E2126–E2133.